Cellular and molecular mechanisms of kidney injury in 2,8-dihydroxyadenine nephropathy

Barbara Mara Klinkhammer[1], Sonja Djudjaj[1], Uta Kunter[2], Runolfur Palsson[3,4], Vidar Orn Edvardsson[4,5], Thorsten Wiech[6], Margret Thorsteinsdottir[7], Sverrir Hardarson[8], Orestes Foresto-Neto[9], Shrikant R. Mulay[9], Marcus Johannes Moeller[2], Wilhelm Jahnen-Dechent[10], Jürgen Floege[2], Hans-Joachim Anders[9], Peter Boor[1,2,11]

1 Institute of Pathology, RWTH University Hospital Aachen, Aachen, Germany

2 Division of Nephrology and Immunology, RWTH University Hospital Aachen, Aachen, Germany

3 Division of Nephrology, Landspitali–The National University Hospital of Iceland, Reykjavik, Iceland

4 Faculty of Medicine, University of Iceland, Reykjavik, Iceland

5 Children´s Medical Center, Landspitali–The National University Hospital of Iceland, Reykjavik, Iceland

6 Institute of Pathology, University Hospital Hamburg-Eppendorf, Hamburg, Germany

7 Faculty of Pharmaceutical Sciences, University of Iceland, Hofsvallagata 53, 107 Reykjavik, Iceland

8 Department of Pathology Landspitali–The National University Hospital of Iceland, Reykjavik, Iceland

9 Division of Nephrology, Klinikum der Universität, LMU München, Munich, Germany

10 Biointerface Laboratory, Helmholtz Institute for Biomedical Engineering, RWTH University Hospital Aachen, Aachen, Germany

11 Department of Electron Microscopy, RWTH University Hospital Aachen, Aachen, Germany

Supplementary material

Table of content

Supplementary Table 1: Blood pressure and laboratory blood and urine parameters of mice with 2,8-DHA nephropathy.

First row shows mean±SD, second row shows median. * p < 0.05 vs. day 1.

0.2% adenine-diet in mice n=4/group	Day 1	Day 3	Day 5	Day 7	Day 14	Day 21	Day 28
blood pressure (systolic / diastolic) [mmHg]	111 / 75	133 / 97	125 / 82	146 / 107 *	151 / 112 *	166 / 124 *	172 / 122 *
s-urea [mmol/l]	15±5 13.7	15±2 15.4	16±2 16.6	22±5 20.8	26±6 25.4	71±16 * 78.4	59±14 * 59.7
s-creatinine [µmol/l]	19±5 17.5	22±2 21.5	22±5 22.5	31±4 31	34±12 36	81±16 * 80	69±13 * 68
s-calcium [mmol/l]	2.6±0 2.6	2.5±0 2.5	2.2±0.3 * 2.2	2.3±0 2.3	2.5±0,1 2.5	2.3±0.2 2.3	2.6±0.2 2.6
anorg. s-phosphate [mmol/l]	1.7±0.3 1.7	1.9±0.1 1.9	2.0±0.6 1.9	2.0±0.5 1.9	2.4±0.5 2.4	5.2±1.9 * 6.2	4.0±1.3 * 3.9
creatinine clearance [ml/24h]	365±140 363	176±138 * 144	147±54 * 144	67±16 * 72	90±91 * 60	30±19 * 25	31±14 * 35
urine volume [ml/24h]	4.02±1.19 4.07	2.01±1.15 1.47	2.11±1.19 1.73	1.18±0.16 * 1.18	1.81±0.76 * 1.47	2.74±1.33 2.69	2.54±1.34 2.69
proteinuria [mg/24h]	1.21±0.81 1.35	0.97±0.52 0.75	0.36±0.20 * 0.38	0.08±0.20 * 0.08	0.09±0.04 * 0.07	0.14±0.07 * 0.13	0.13±0.07 * 0.13
urinary DHA excretion [µg/24h]	384±208 381	50±13 * 48	55±11 * 56	35±24 * 28	55±33 * 45	53±21 * 52	43±18 * 44
platelets [x10^3/µl]	1173±170 1199	1124±114 1105	1384±219 1348	1612±229 1604	1171±181 1162	1859±148 1896	1275±150 1320
Erythrocytes [x10^6/µl]	9.4±0.3 9.4	9.4±0.1 9.4	9.3±0.4 9.2	9.3±0.6 9.1	10.5±1.4 10.4	9±0.3 9.2	9.1±2.2 8.3
Leukocytes [x10^3/µl]	9250±4713	3600±1742	2475±772	3200±1924	6800±2221	1900±529	3550±700
banded neutros [%]	3,5±1,7	5±0,8	3,5±2,4	3,8±1,7	2,5±1,3	4,0±1,7	3,8±1,7
segmented neutros [%]	29±9,9	41±11,2	42±14,6	53±17,9	32±8,2	44±13,9	35±7,5
lymphocytes [%]	57±10,3	45±11,6	44±14,8	35±17,0	55±14,9	43±10,1	48±7,7
monocytes [%]	7,3±3,2	5,8±2,9	6,3±2,9	6,8±1,3	8,3±3,9	7,3±3,1	10,8±0,5
eosinophils [%]	3,5±1,3	3,0±2,2	4,5±1,3	2,0±1,1	2,5±2,5	1,3±0,6	3,0±2,2
basophils [%]	0±0	0±0	0±0	0±0	0±0	0±0	0±0

Supplementary Table 2: Comparison of young and aged mice with 2,8-DHA nephropathy.

A group of 10-12-week-old male mice fed with 0.2% adenine diet (comprising the day 21 group from time course experiment and day 21 group from fluid intake therapy experiment) was compared to aged male mice fed the same adenine-enriched diet day 21 mice. We found no differences for kidney function, 2,8-DHA crystal deposition of renal injury.

Adenine day 21	s-urea [mmol/l]	s-creatinine [µmol/l]	creatinine clearance [ml/24 h]	renal 2,8-DHA crystals [area %]	Tubulointerstitial injury
Young	53±20	77±16	38±19	1.0±0.4	3.6±0.5
Old	35±11	71±25	70±45	1.1±0.1	3.2±0.3

Supplementary Table 3: Kidney function in rats with 2,8-dihydroxyadenine nephropathy.

* $p < 0.05$ vs. pre-adenine-enriched diet.

	s-urea [mmol/l]	**s-creatinine [µmol/l]**	**anorg. s-phosphate [mmol/l]**	**s-calcium [mmol/l]**
Pre-adenine-enriched diet (n=9)	5,5 ± 0.3	32 ± 3	2.8 ± 0.2	2.7 ± 0.1
day 14 (n=3)	42 ± 0.9 *	195 ± 7 *	4.6 ± 0.8 *	2.9 ± 0.1 *
day 21 (n=3)	42 ± 2.1 *	244 ± 56 *	3.9 ± 0.5	2.7 ± 0.1
day 28 (n=3)	45 ± 5.4 *	273 ± 33 *	4.9 ± 0.5 *	2.8 ± 0

Supplementary Table 4: Summary of performed mouse experiments.

↔ no change, ↘ slightly decreased, ↗ slightly increased, ↓ decreased, ↑ increased, ↓***** significantly decreased compared to control.

Anxa2 (annexin A2), Lcn2 (lipocalin-2), n.a. (not analyzed), TI (tubulointerstitial).

	♀ **vs.** ♂	***Tnfr1*$^{-/-}$**	***Tnfr2*$^{-/-}$**	***Cd44*$^{-/-}$**	***Ahsg*$^{-/-}$**
s-urea [mmol/l]	↓	↓*****	↔	↘	↔
s-creatinine [µmol/l]	↓	↓	↗	↘	↔
creatinine clearance [ml/24h]	↔	n.a.	n.a.	↔	↔
blood pressure (systolic) [mmHg]	↔	n.a.	n.a.	↘	↔
Lcn2 / *Lcn2*	↓*****	↓	↓	↗	↗
Anxa2	n.a.	↓*****	↘	↔	↔
CD44 / *Cd44*	n.a.	↓*****	↔	↓*****	↗
Crystals [area]	↓*****	↓*****	↘	↓*****	↔
TI injury	↔	↓*****	↔	↔	↔
F4/80	↘	↓*****	↓	↓*****	↔
αSMA/SM22α	↘	↔	↑	↔	↘
Col. III	↔	↓*****	↔	↘	↔

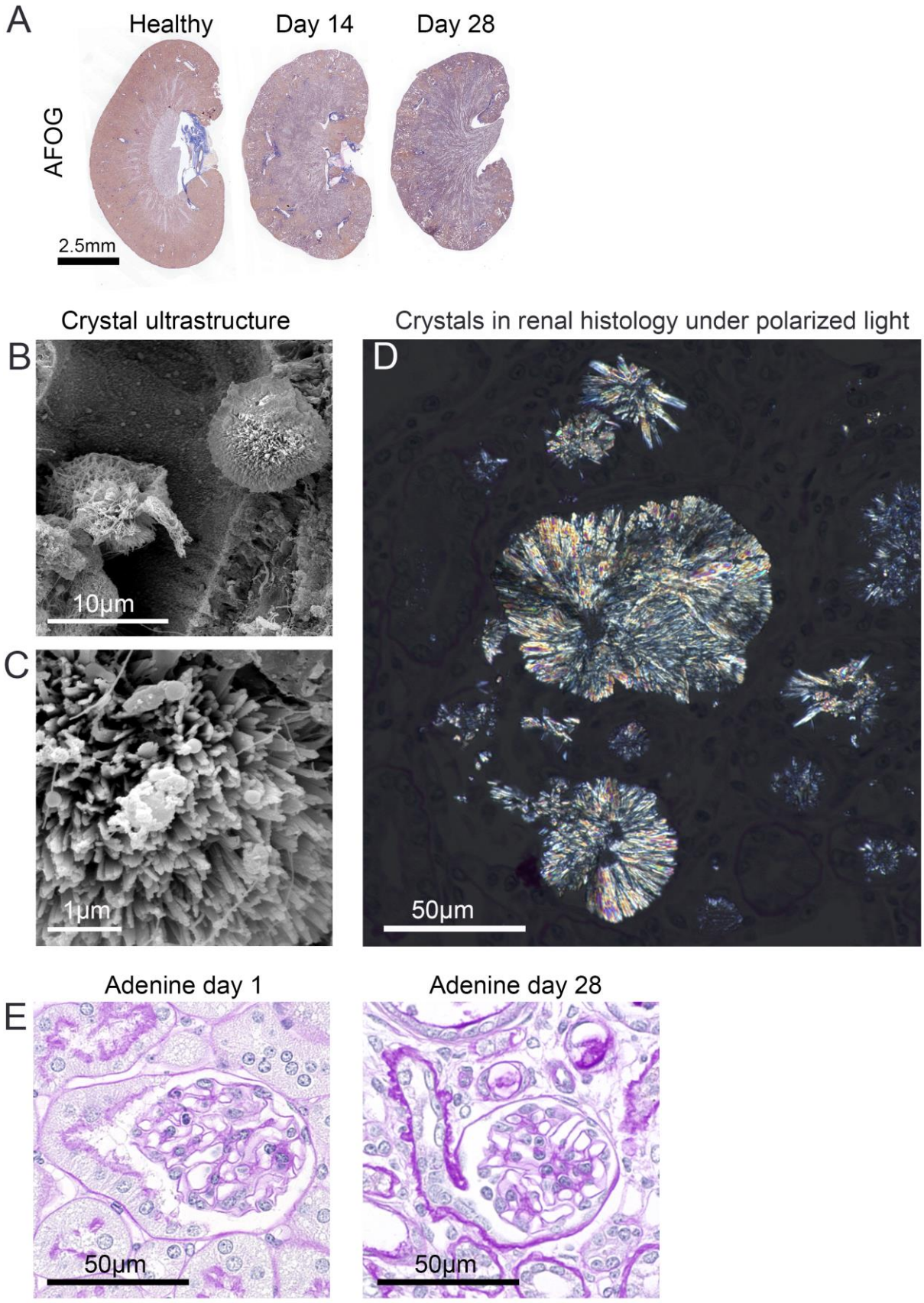

Supp. Figure 1: Basic characteristics of the rodent 2,8-dihydroxyadenine nephropathy model. (A) AFOG-stained kidney cross sections from healthy mice and mice fed with 0.2% adenine diet for 14 and 28 days (B+C). Ultrastructure of 2,8-DHA crystals in rat kidney. (D) 2,8-DHA crystals in renal histology sections were birefringent when viewed by polarized light, showing spiky appearance. (E) PAS sections showed that glomeruli were not affected in mice with adenine nephropathy in contrast to tubules.

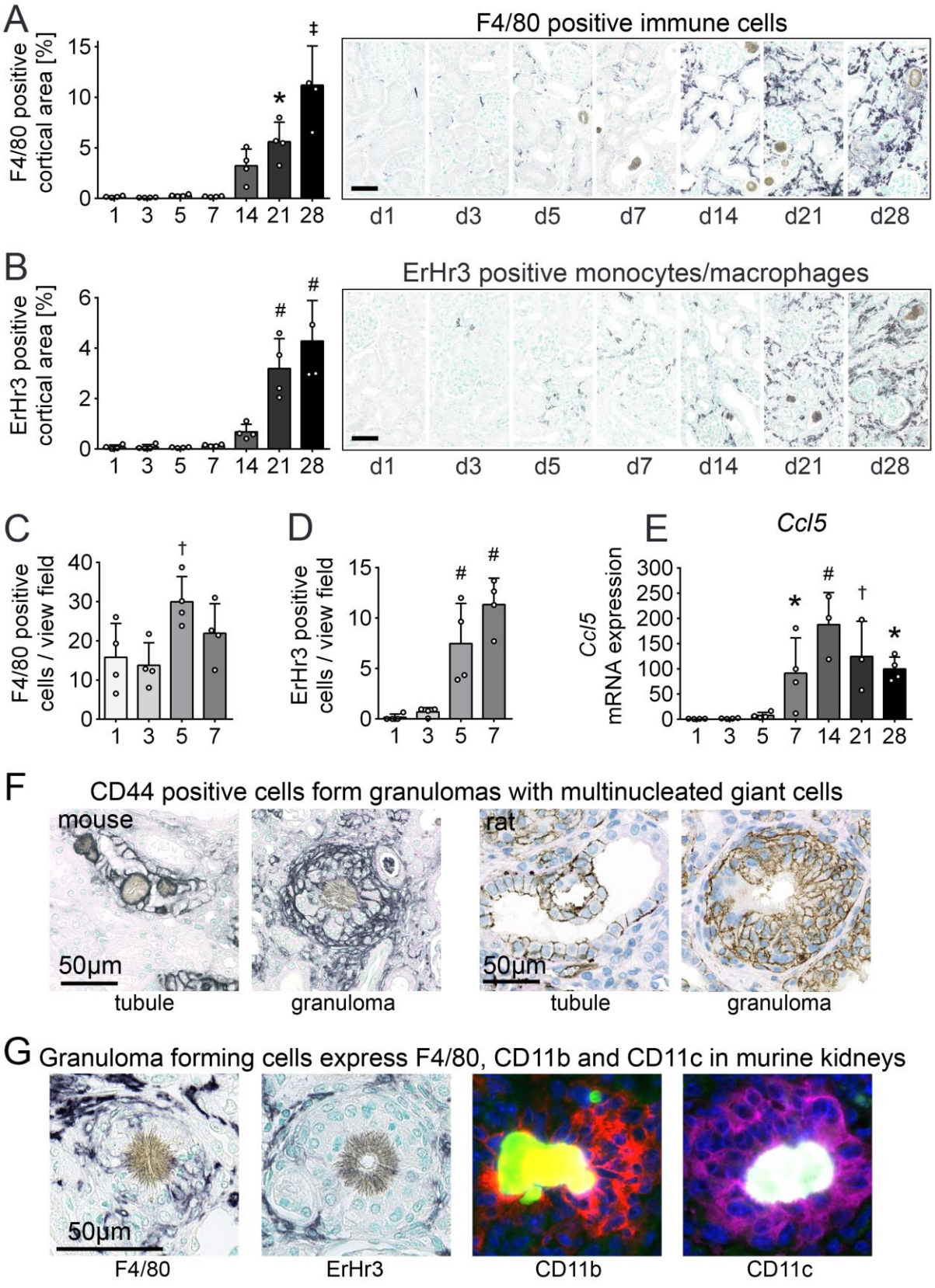

Supp. Figure 2: 2,8-DHA nephropathy is characterized by massive inflammation in mice and rats.

Expression of F4/80 (A) and ErHr3 (B) analyzed by immunohistochemistry in kidney sections harvested following time-course experiments in mice fed with 0.2% adenine diet (n=4/group). (C) Results from computer-assisted morphometric quantification analyses and from single-cell counting in the same histologies (D) illustrated an increase of immune cells already from day 5 on. The mRNA expression of the chemokine *Ccl5* was significantly upregulated during the time course (E). CD44 was expressed in mice and rats with 2,8-dihydroxyadenine nephropathy, with tubular cells and interstitial immune cells forming granuloma (F). Further stainings of mouse kidney tissue characterized the interstitial crystal-degrading granulomas which are composed of multinucleated giant cells expressing F4/80, CD11b and CD11c but minimally ErHr3 (G). Scale bars represent 50 µm. * p<0.05, † * p<0.01, ‡ p<0.001, # p<0.0001 vs day1.

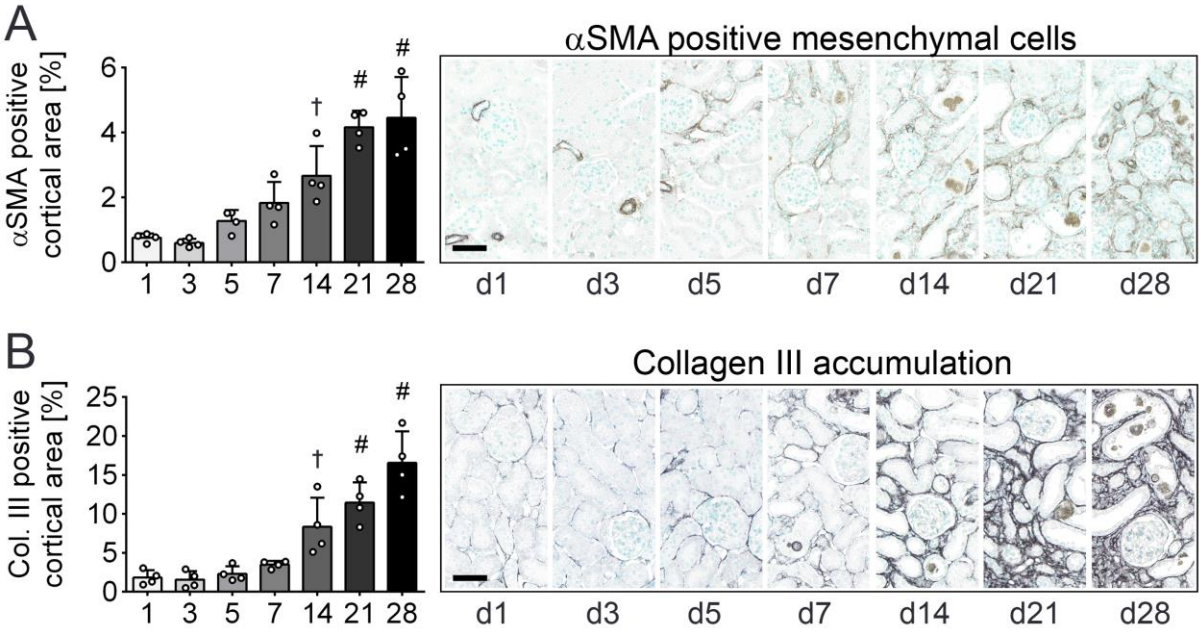

Supp. Figure 3: 2,8-DHA nephropathy is characterized by progressive renal fibrosis in mice. During the adenine-enriched diet time course (n=4/group), development of fibrosis was quantified on immunohistochemically stained kidney sections. The area positively stained for myofibroblast marker αSMA (A) significantly increased and, similarly, the extracellular matrix represented by collagen III (B). Scale bars represent 50 µm. * $p<0.05$, † * $p<0.01$, ‡ $p<0.001$, # $p<0.0001$ vs day1.

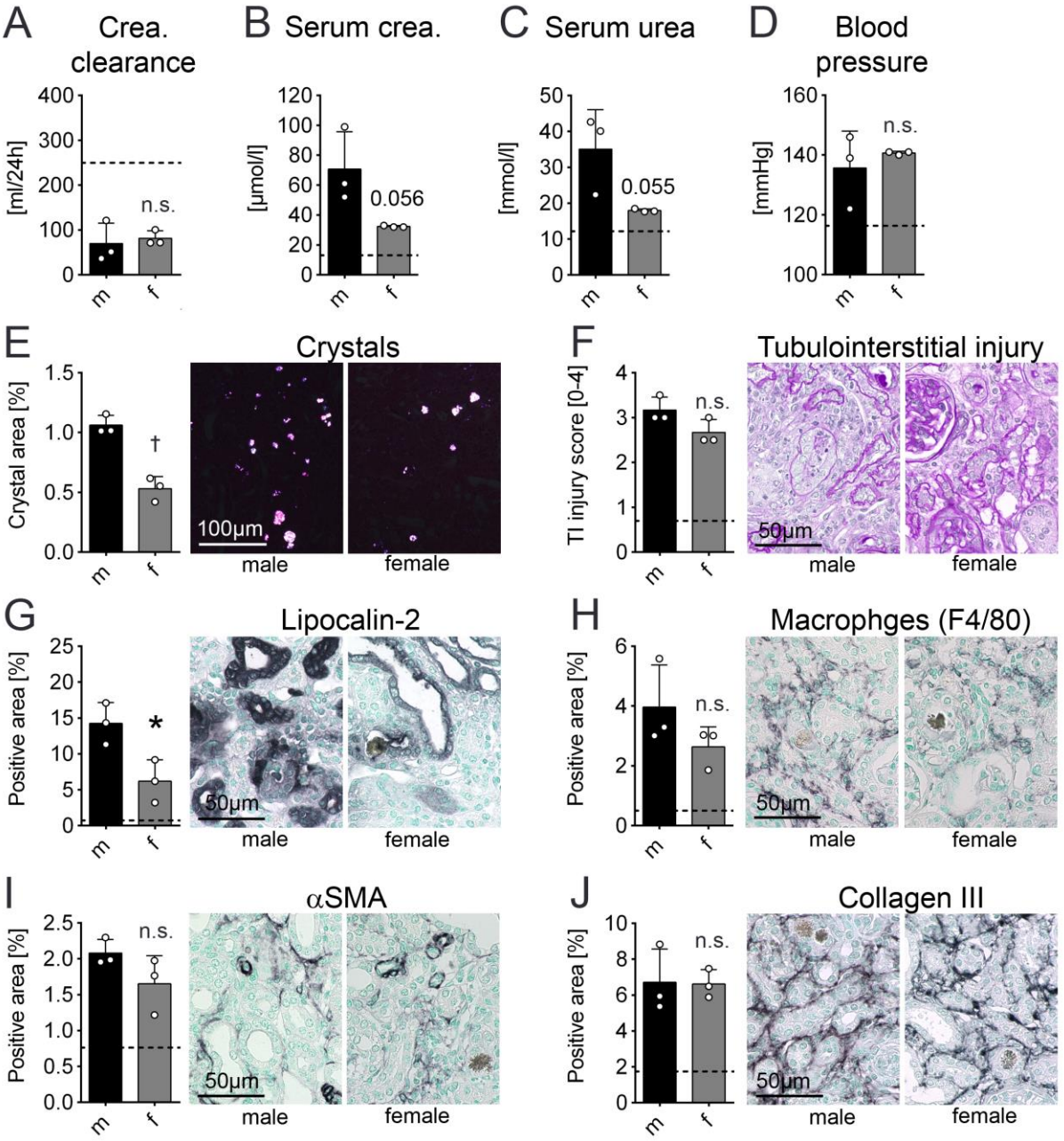

Supp. Figure 4: 2,8-DHA nephropathy in aging mice.

Kidney function analyzed by creatinine clearance (A), serum creatinine (B), serum urea (C) and systolic blood pressure (D) did not differ between male and female mice that received 0.2% adenine diet. Female mice exhibited lower 2,8-DHA crystal deposition (~~D~~E) but similar tubulointerstitial injury (~~E~~F) compared to male littermates. Expression of the tubular injury marker lipocalin-2 was significantly lower in female mice (~~F~~G). There was no difference between males and female animals regarding macrophage infiltration (~~G~~H), αSMA expression (~~H~~I) or collagen III deposition (~~I~~J). Scale bars indicate 50 or 100 µm, respectively. * p<0.05, † * p<0.01, ‡ p<0.001, # p<0.0001.

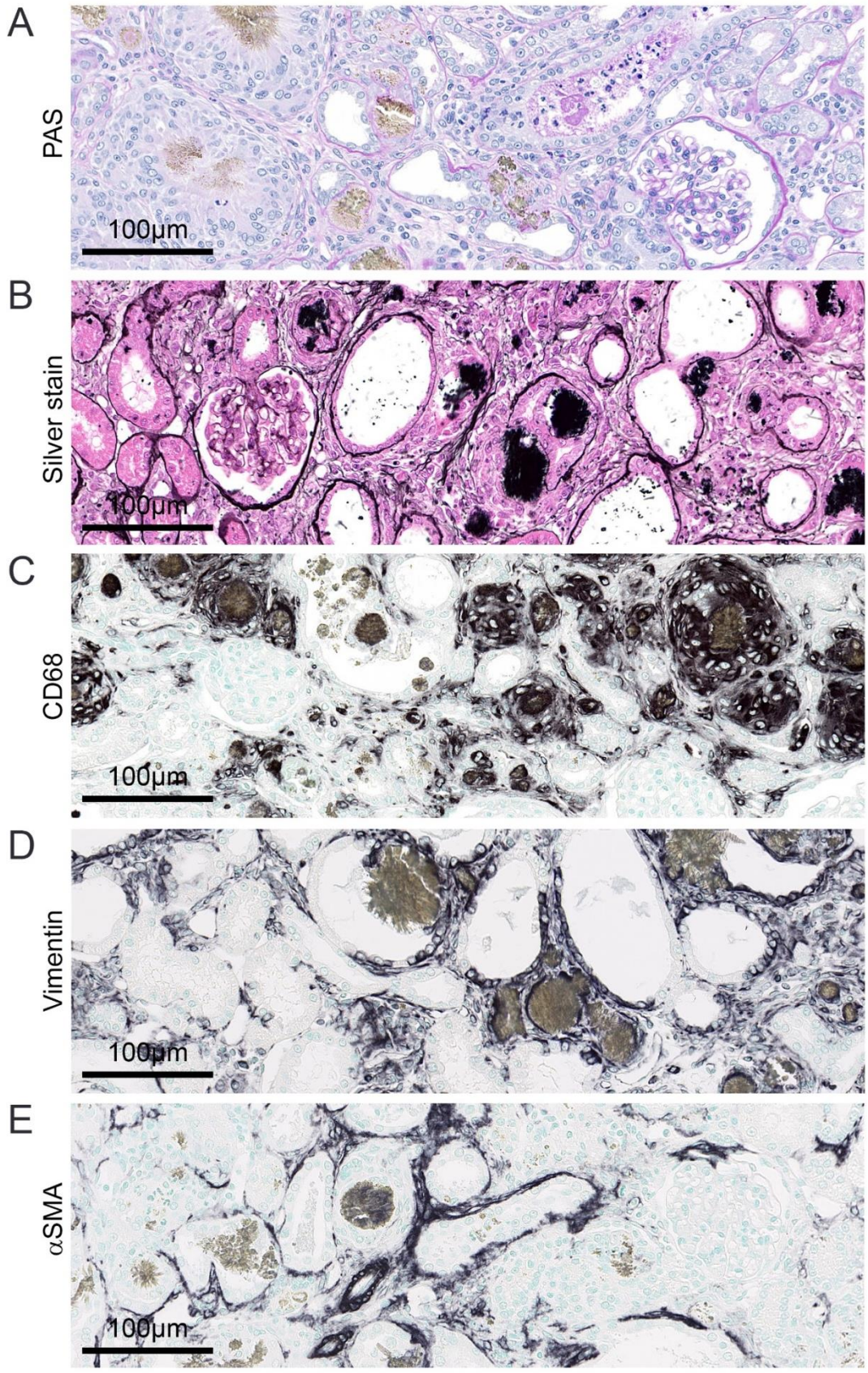

Supp. Figure 5: 2,8-DHA nephropathy in rats.
Depicted are kidney sections from a rats fed 0.75% adenine diet for 21 days stained with PAS (A), methenamine silver (B) and immunohistochemistry for CD68 as macrophage marker (C), vimentin as mesenchymal marker (D) and αSMA as myofibroblast marker (E). Brownish 2,8-DHA crystals were associated with similar kidney damage in the rats as in mice. Scale bars indicate 100 µm.

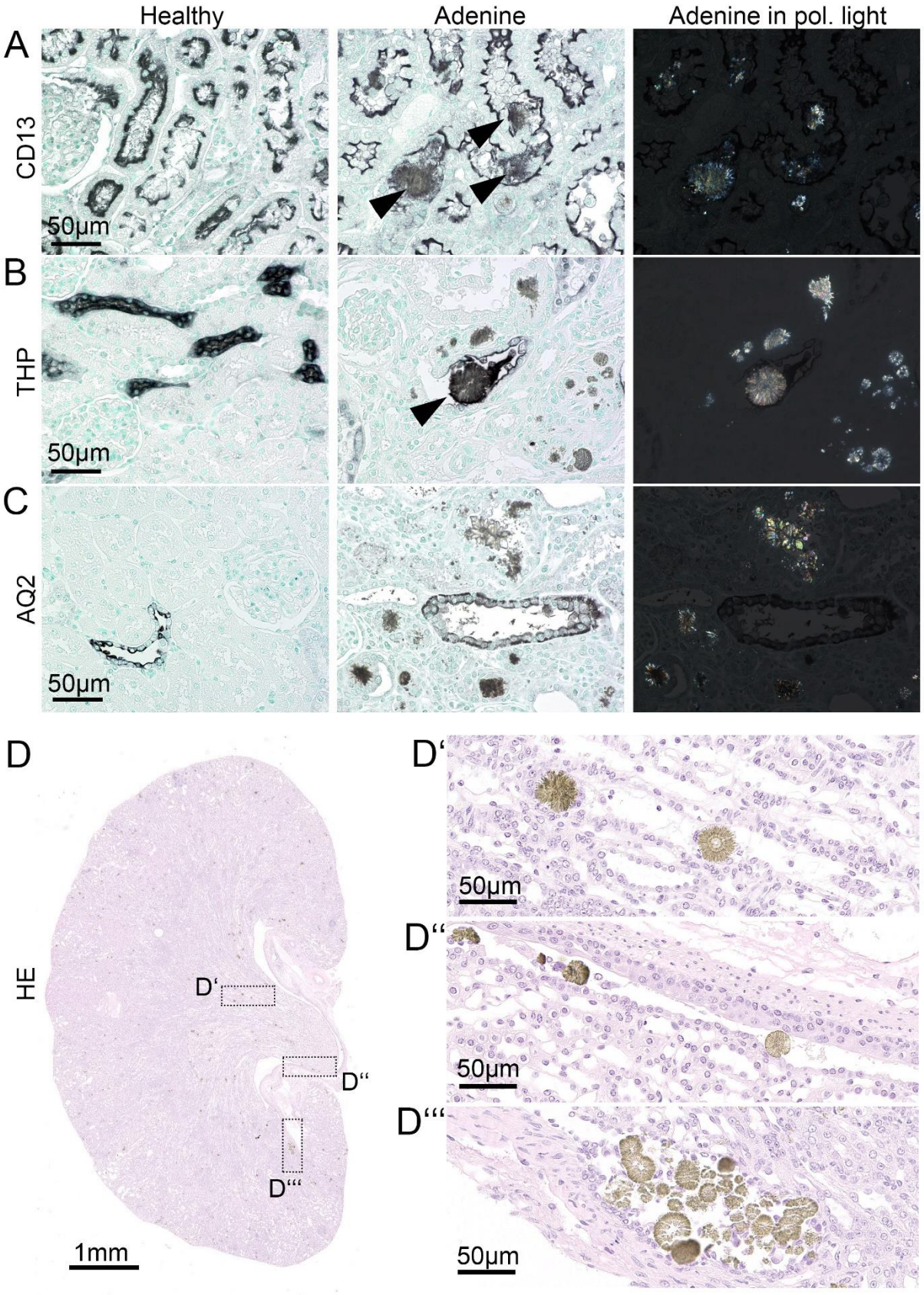

Supp. Figure 6: Location of intrarenal 2,8-DHA crystals in rats and mice.
Immunohistochemical stainings for CD13 (A), THP (B) and AQ2 (C). The left panel shows healthy rat kidney, the middle panel kidney from rat fed 0.75% adenine diet and the right panel highlights the 2,8-DHA crystals viewed by polarized light microscopy. Crystals (arrowheads) were mainly located and adherent in $CD13^+$ proximal tubules and in the THP^+ segment, but not in $AQ2^+$ collecting ducts. HE staining of a mouse adenine kidney (D) confirmed the location of crystals in the loop of Henle (D') and also visualized crystals adherent to the urothelium in the renal pelvis (D''+D'''). THP = Tamm-Horsfall protein, AQ2 = Aquaporin-2. Scale bars indicate 50 µm or 1 mm, respectively.

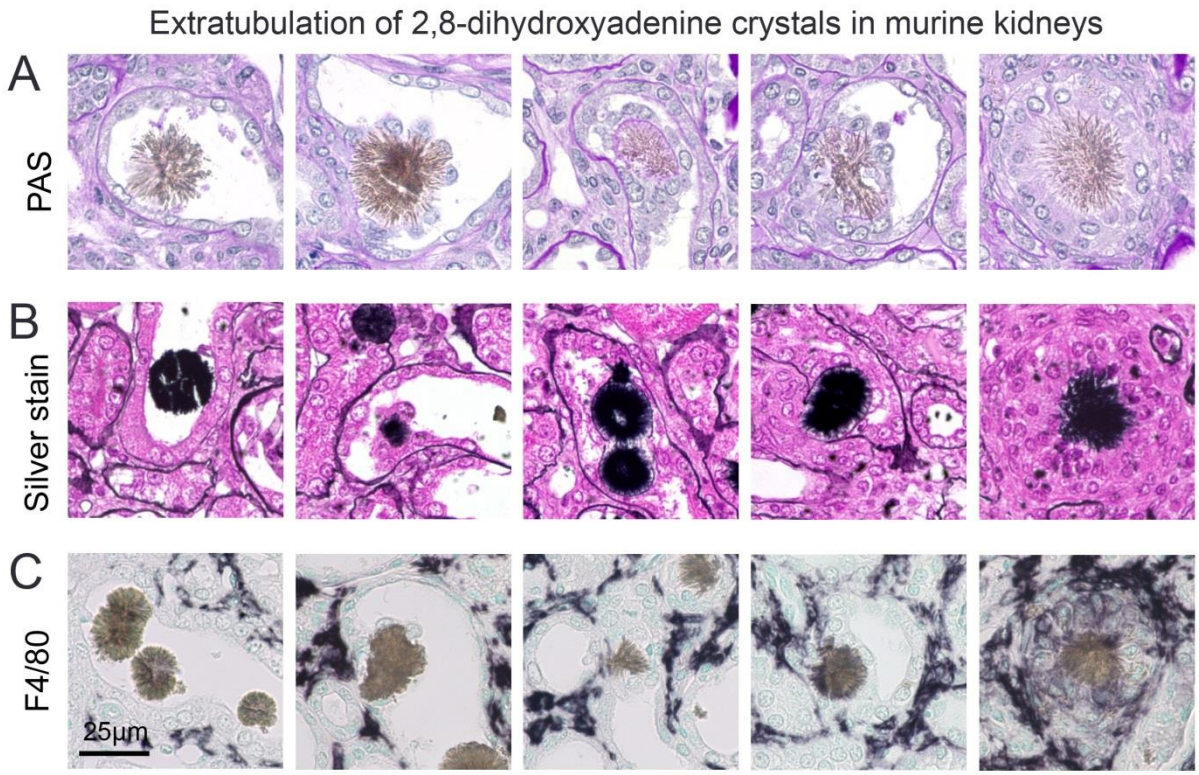

Supp. Figure 7: Extratubulation in mouse kidneys.

The process of extratubulation in murine adenine kidneys is shown in kidney sections stained with PAS (A), methenamine silver (B) and F4/80 immunohistochemistry (C). Scale bar indicates 25 µm.

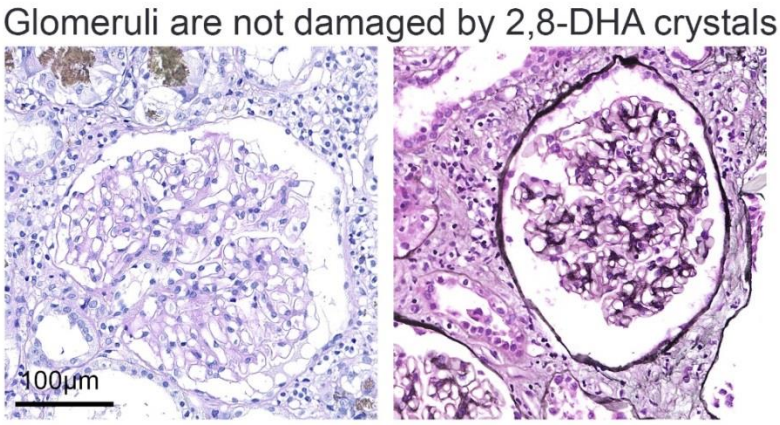

Supp. Figure 8: In patients with APRT deficiency, renal glomeruli are not directly affected by the crystal nephropathy.

The glomeruli stained with PAS (left panel) or silver staining (right panel) did not show 2,8-DHA crystal deposits or other pathologic features.

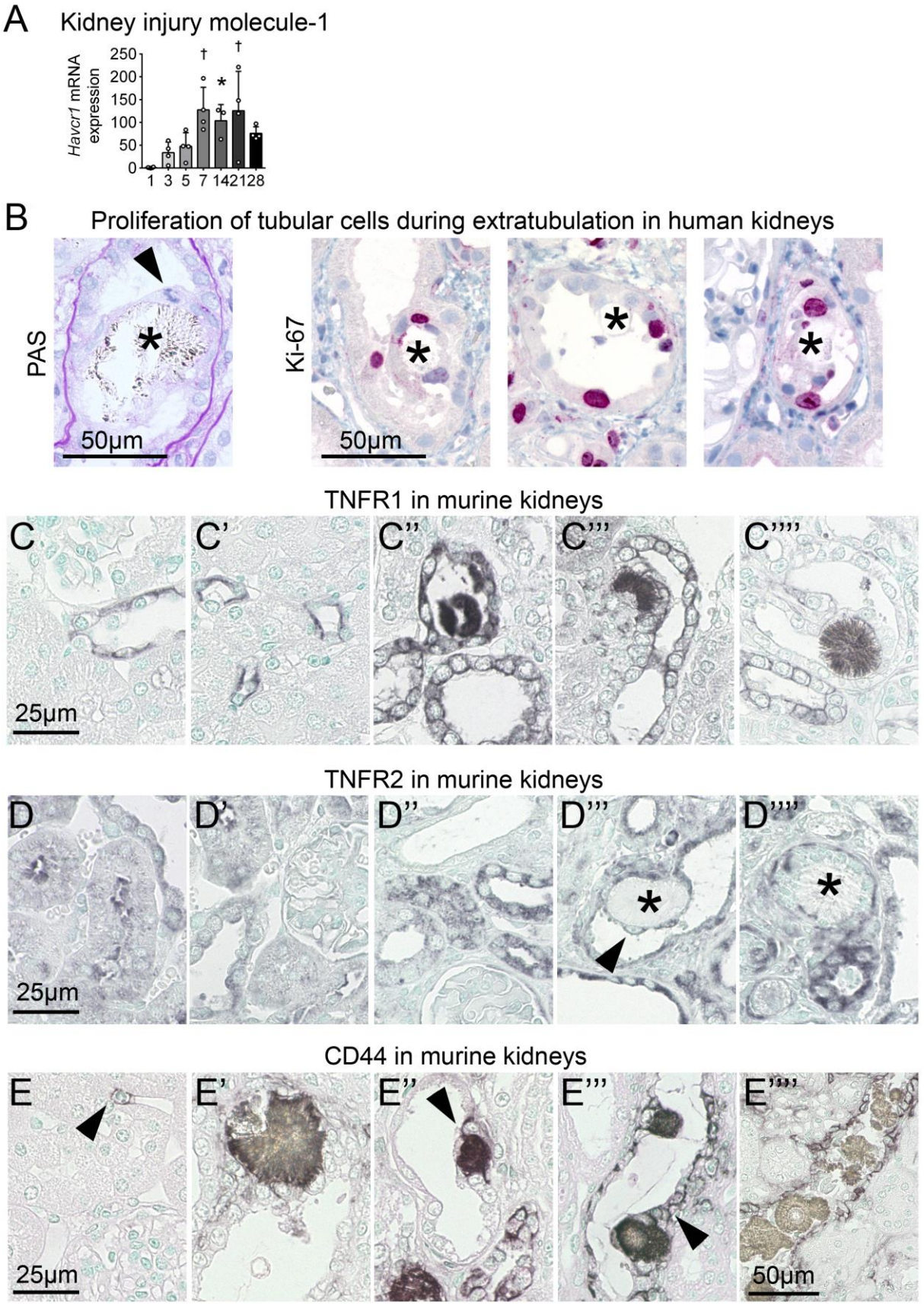

Supp. Figure 9: Characterization of tubular phenotype in murine and human 2,8-DHA nephropathy.

(A) mRNA expression of *Havcr1* (KIM-1) in adenine time course (n=4/group). (B) Proliferation of tubular epithelial cells at sites of extratubulating 2,8-DHA crystal (*) shown by mitotic figure in PAS staining (arrowhead) and red immunohistochemical staining for the proliferation marker Ki-67. Immunohistochemistry of murine kidney sections for TNFR1 (C-C''''), TNFR2 (D-D''''), and CD44 (E-E''''). In the healthy kidney, TNFR1 was only expressed at basal and luminal sites of collecting ducts in cortex (C) and medulla (C'). In 2,8-DHA nephropathy, TNFR1 was upregulated and showed a circumferential staining pattern (C''). In many cases, crystals were adherent and extratubulated in $TNFR1^{+}$ tubules (C'''), while extratubulation was occasionally observed in $TNFR1^{-}$ tubules (C'''').

(D+D') TNFR2 in healthy kidneys was expressed in brush borders of proximal tubules and faintly also in collecting ducts while glomeruli remained negative. (D'') In adenine kidneys, TNFR2 was upregulated, showed a cytoplasmic staining pattern. (D'''+D'''') Crystals (stars) were adherent and extratubulated in tubules expressing TNFR2. (E) CD44 was only expressed by a few interstitial cells (arrowhead) in healthy kidneys. 2,8-DHA crystals were adherent in $CD44^-$ (E') as well as $CD44^+$ tubules (E''+E'''). CD44 expression was primarily basolateral or circumferential. (E'''') Urothelium stained positive for CD44 and occasionally showed adherent crystal aggregates. TNFR = Tumor necrosis factor receptor. Scale bars indicate 25 µm or 50 µm, respectively. * $p<0.05$, † $p<0.01$, ‡ $p<0.001$, # $p<0.0001$ vs day1.

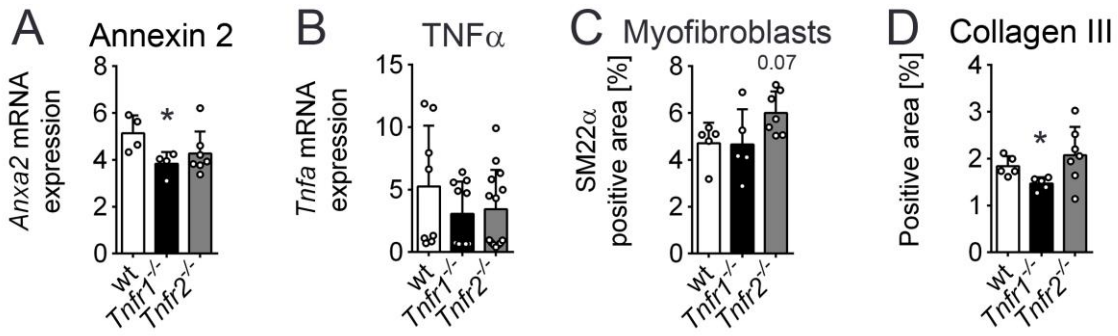

Supp. Figure 10: 2,8-DHA nephropathy in *Tnfr1*$^{-/-}$ and *Tnfr2*$^{-/-}$ mice.

(A) *Anxa2* (Annexin 2) and (B) *Tnfa* mRNA expression. Quantification of immunohistochemical stainings for Sm22α (smooth muscle protein 22-alpha) (C) and collagen III (D). wt = wildtype, * $p<0.05$ vs. wt.

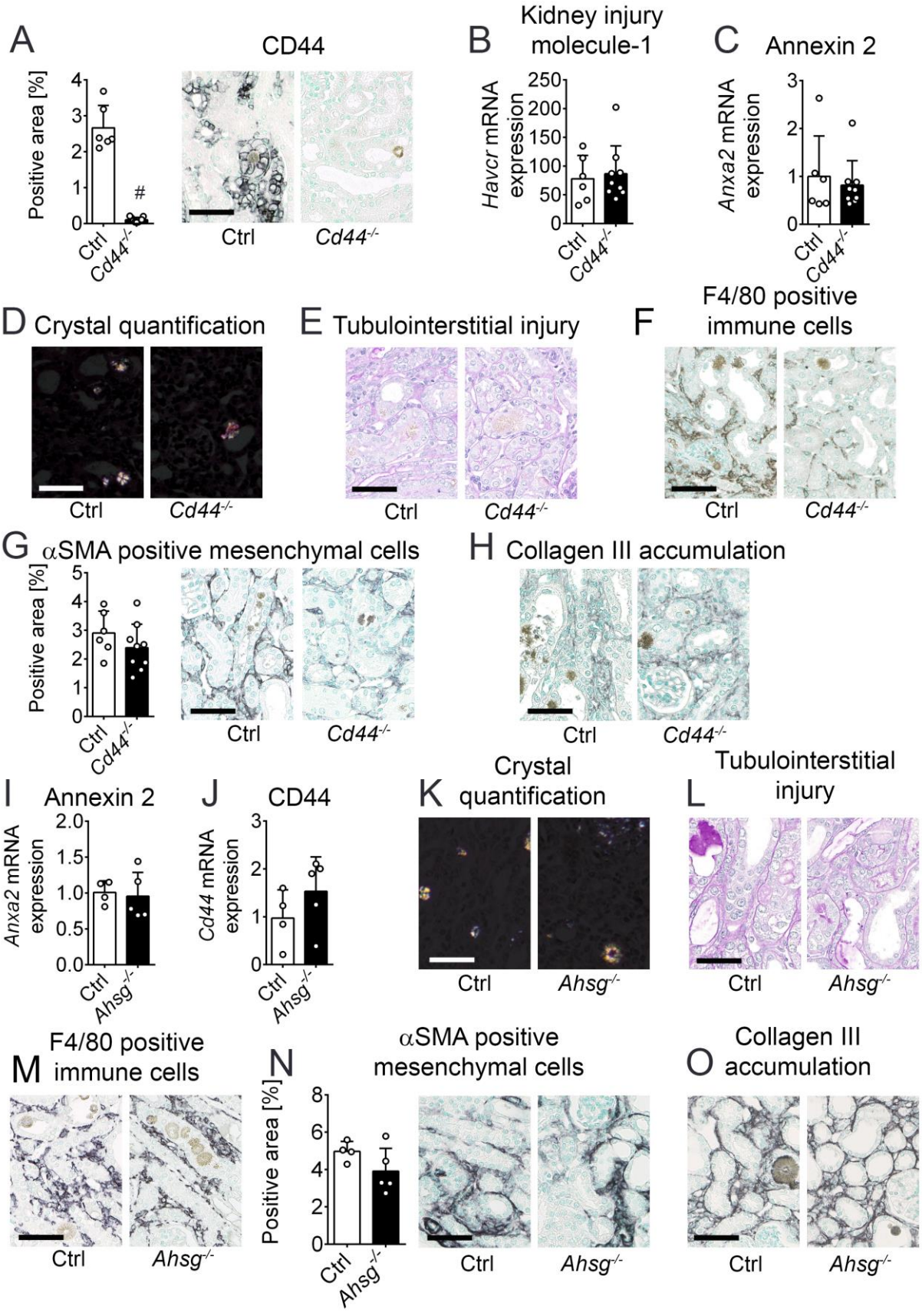

Supp. Figure 11: 2,8-DHA nephropathy in *Cd44*$^{-/-}$ and *Ahsg*$^{-/-}$ mice.

(A) Immunohistochemistry for CD44 confirmed the deletion of CD44 in knockout mice. No difference in *Havcr1* (KIM-1, (B)) or *Anxa2* (Annexin 2 (C)) mRNA expression was detected between *Cd44*$^{+/-}$ and *Cd44*$^{-/-}$ mice. Shown are representative images of sections from *Cd44* mice stained with HE viewed in polarized light (~~C~~D), PAS (~~D~~E) and F4/80 immunohistochemistry (~~E~~F). No differences were detected in expression of αSMA (G) or collagen III (H). No difference in *Anxa2* (I) or *Cd44* (J) expression was detected between *Ahsg*$^{-/-}$ (Fetuin-A) and wildtype mice. Representative images of sections from *Ahsg*$^{-/-}$ ~~(Fetuin-A)~~ mice stained with HE (~~F~~K), PAS (~~G~~L) and F4/80 (~~H~~M). (M) Quantification of αSMA immunohistochemistry yielded similar results for control wildtype mice and *Ahsg*$^{-/-}$ mice. (~~J~~O)

Representative images for collagen type III staining. Ctrl = control, # $p<0.0001$ vs control. Scale bar indicates 50 µm.